Eur. Phys. J. AP **5**, 251–256 (1999)

THE EUROPEAN PHYSICAL JOURNAL APPLIED PHYSICS

Production of carbon nanotubes by the solar route

T. Guillard[1], S. Cetout[2], L. Alvarez[2], J.L. Sauvajol[2], E. Anglaret[2], P. Bernier[2], G. Flamant[1], and D. Laplaze[2,a]

[1] Institut de Sciences et de Génie des Matériaux et Procédés, Centre du Four Solaire Félix Trombe, B.P. 5, Odeillo, 66125 Font-Romeu Cedex, France

[2] Groupe de Dynamique des Phases Condensées, Université de Montpellier II, 34095 Montpellier Cedex 5, France

Received: 17 June 1998 / Revised: 13 November 1998 / Accepted: 17 December 1998

Abstract. The high intensity of concentrated solar radiation obtained with the Odeillo (France) solar furnace facilities can be used to produce carbon nanotubes by direct vaporization of carbon bi-metal targets under inert gas atmosphere. Electron microscope pictures and Raman spectra show that the structure of the produced carbon nanotubes is likely to depend on experimental conditions and that the growth of single-wall or multi-walled carbon nanotubes can be favored.

Résumé. La forte concentration du rayonnement solaire que l'on peut obtenir grâce aux installations du centre du four solaire d'Odeillo (France) nous a permis de synthétiser des nanotubes de carbone par la méthode de vaporisation-condensation en présence de gaz inerte (argon). Les observations en microscopie électronique (MEB et TEM) ainsi que l'analyse des spectres Raman montrent que la structure des nanotubes de carbone obtenus dépend fortement des conditions expérimentales et que l'on peut favoriser la croissance de nanotubes d'un type déterminé (monofeuillets ou multifeuillets) en modifiant les paramètres de synthèse.

PACS. 61.46.+w Clusters, nanoparticles, and nanocrystalline materials – 81.05.-t Specific materials: fabrication, treatment, testing and analysis – 81.10.Bk Growth from vapor

1 Introduction

The vaporization-condensation method performed in highly concentrated sunlight for the production of fullerenes [1] has been successfully used for the production of carbon nanotubes [2]. All these tests have been performed with a vertical 2 kW solar furnace at the Odeillo Institute. This small-scale experimental set-up limits the target size and yields a small amount of material due to the low power of the solar furnace and the small size of the focus area. However, it is well-designed to perform accurate analysis of the evolution of the structure of the produced material with various synthesis parameters. The more important limiting factor is the vaporization temperature which remains too low to obtain high purity carbon nanotubes. The samples prepared by the solar method contain undesired nanoparticles in a larger amount than the ones prepared by electric-arc.

2 Experimental set-up

The experimental set-up is the same as the one used for solar fullerene production and has been previously described [1,2]. Briefly, it is composed of a Pyrex spherical chamber linked to a water cooled stand (Fig. 1). For the production of carbon nanotubes, the target material is a mixture of powdered graphite and catalysts. The mixture is placed in a graphite crucible located in the center of the chamber and this crucible is surrounded by a graphite pipe which canalizes the vapor and acts like a thermal screen. When the crucible is placed at the focus of the 2 kW solar furnace, the temperature can reach 2950–3000 K which is high enough to vaporize the mixture under an argon atmosphere.

The target temperature has been measured with a Heimann pyrometer equipped with an interferential filter centered at 2.7 μm. It was focussed to the target through a LiF window as shown in the inset of Figure 1. At this wave length, we observe only the emission of the target as the glass of the tracking mirror absorb all the sun radiation of wave length greater than 2 μm. These measurements have shown that the graphite pipe produce an increase of the target temperature greater than 150 K.

In the first series of experiments we vaporized a mixture of powdered graphite, nickel and cobalt (4 at.% metal in C with Ni:Co ratio of 1:1) to study the effects of the synthesis parameters. Further tests were performed with different compositions of the target to probe the effects of catalyst elements.

The produced material is mainly condensed into the graphite pipe. It has a rubbery aspect when carbon nanotubes are produced and large sheets can be easily pulled

[a] e-mail: laplaze@gdpc.univ-montp2.fr

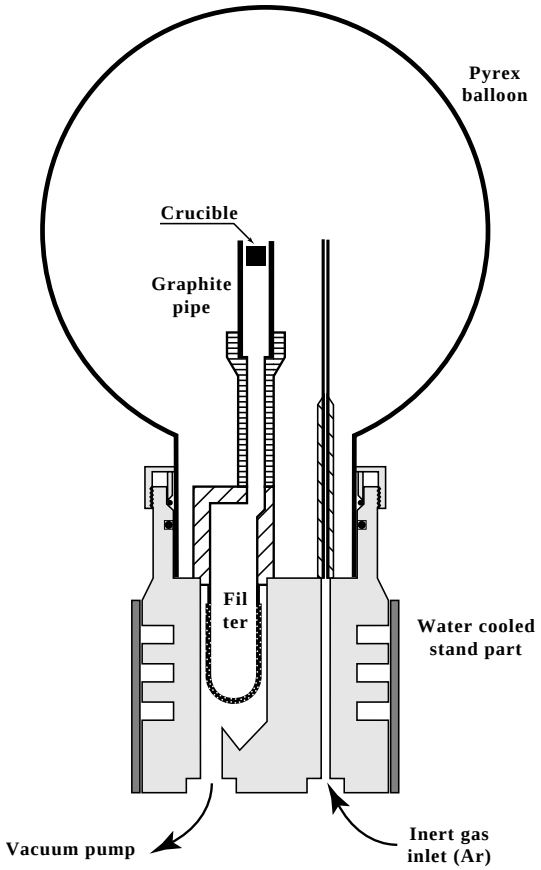

Fig. 1. Schematic diagram of the reactor. For carbon nanotube production the mixture of powdered graphite and catalysts is put in a graphite crucible surrounded by the graphite pipe. The inset shows the arrangement for the measurement of the target temperature.

off. This material also contains catalyst nanoparticles embedded in amorphous carbon, empty carbon vesicles and amorphous carbon. The homogeneity and purity of the as grown soot is likely dependent on the synthesis parameters: the vaporization temperature ($T_{\rm v}$), the pressure and flow rate of argon gas, and the target composition.

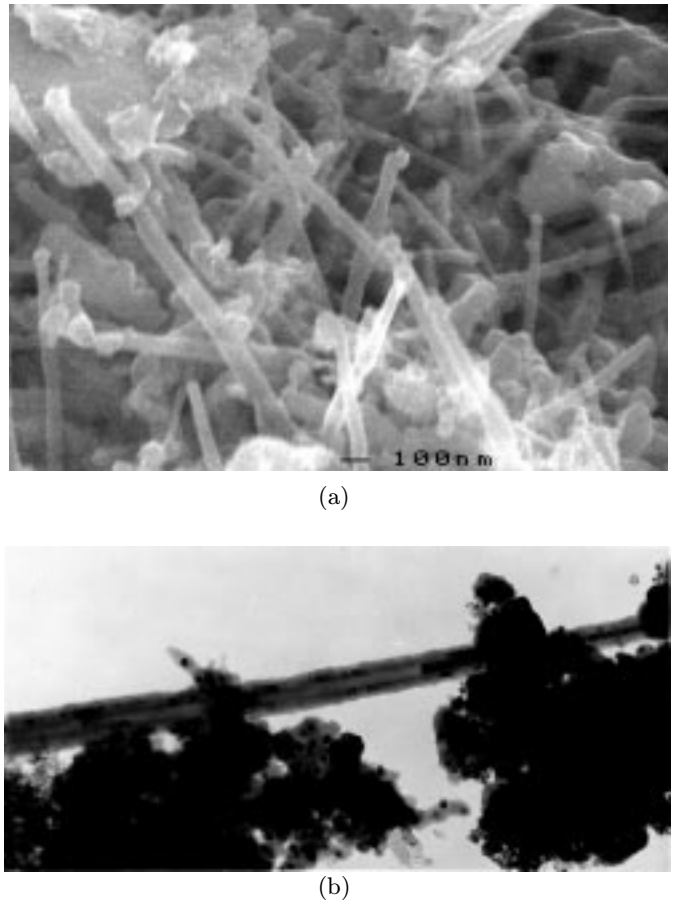

Fig. 2. SEM (a) and TEM (b) pictures of soot produced at low pressure (120 mbar). The atomic target composition is 96% C, 2% Co and 2% Ni. We only observe carbon fibrils and nanoparticles.

3 Target temperature, pressure and flow rate

The most important parameter is the vaporization temperature, $T_{\rm v}$, which currently reaches 2950 K with the 2 kW solar furnace. At lower $T_{\rm v}$, the production of nanotubes is weak and the purity of the material is poor. To obtain larger amounts of better purity carbon nanotubes it will be necessary to vaporize the target at temperatures near 3300 K and this goal can be obtained with a larger furnace [3]. Nevertheless, with a clear sky condition ($T_{\rm v} \sim 2950$ K) one can vaporize the 100 mg of mixture contained in the crucible in 10 mn. By collecting the sheets produced during several runs performed with the same conditions, one can easily obtain some hundreds of milligrams of material in a day, which is enough to observe the structure evolution as a function of experimental conditions.

From the set of experiments carried out with the same $T_{\rm v}$, we have observed that the structure of the produced nanotubes changes with the pressure. Electron microscopy (SEM and TEM) illustrations are reported in the Figures 2, 3 and 4. For SEM microscopy, samples are sticked

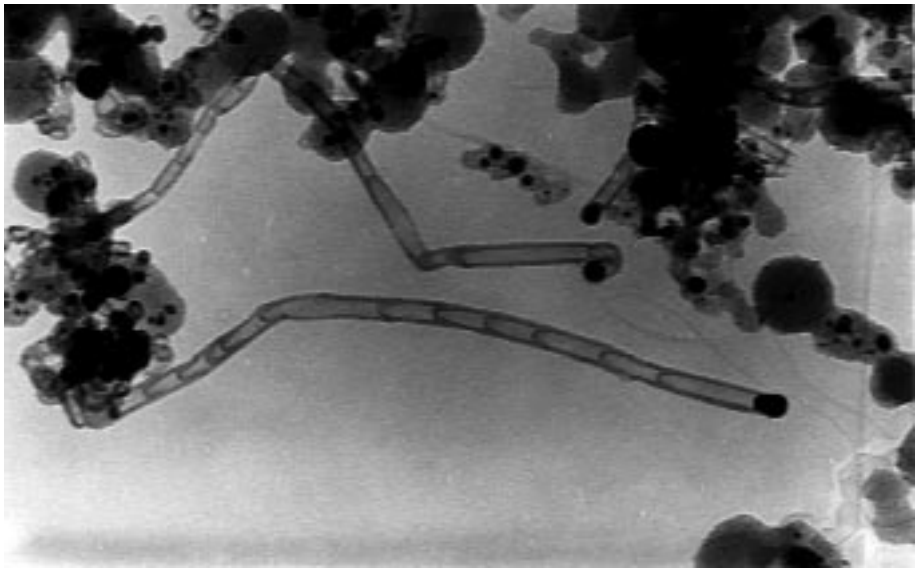

Fig. 3. At medium pressure (250 mbar) and for the same mixture composition as in Figure 2, we observe large amount of multi-walled nanotubes. Many of them show the presence of a catalyst nanoparticles at the end of the tube.

on a metallic support with a carbon conducting film and covered with a very thin platinium film (10–15 A). For TEM, the samples were sonicated in ethanol and a drop of material was deposited on a copper grid covered with a holey carbon film. At low pressure (120 mbar) we do not observe nanotubes but, in some cases, are observed large fibrils which look like precursors of carbon fibers. When the pressure reaches 250 mbar, the samples contain large amounts of bamboo-like multi-walled nanotubes, and we begin to find a few small ropes of single-wall nanotubes. The large fibrils observed at low pressure can also be observed. At higher pressure (400–600 mbar) no multiwalled nanotubes was observed in TEM images. Only bundles of single wall nanotubes were observed, some of them containing a large number of nanotubes.

These results are consistent with the proposed growth mechanisms of carbon nanotubes [4–6]. An increase of the pressure produces a dilution of the vaporized carbon atoms and prevents their fast and disordered clustering, favoring the growth of ordered structures. The pressure dependence of the structure of the carbonaceous deposit has also been observed during laser ablation experiments by Yudasaka *et al.* [7] who pointed out the possible effect of the pressure on the vaporization of the catalysts.

Similar dilution effects can be obtained at constant pressure and vaporization rate by changing the flow rate of the gas. But in this case we also change the residence time of the carbon vapor in the hot part of the reactor. We observed that the increase of the flow rate leads to a larger amount of undesired nanoparticles and amorphous carbon. Such an increase of the cooling rate can also induce modifications of the size of the catalyst nanoparticles and can favor the production of multi-walled nanotubes, especially at low pressure. The other point one must note is that the temperature decreases very rapidly along the graphite pipe where the sheets of nanotubes are condensed and in some cases we have pulled off sheets longer than 3 cm. For the same experiment, samples collected at different distances from the top of the pipe contain the same kind of nanotubes. The quantity of amorphous carbon and nanoparticles is generally greater for the samples collected in the colder part of the pipe and generally we do not find nanotubes in the filter. From these observations, we can assume that carbon nanotubes grow in the high temperature zone of the reactor which is close to the crucible. Turbulent flow which occurs through the weak annular aperture between the pipe and the back of the crucible favor the tube deposition. As a consequence, a reduction of the temperature gradient could improve the process and lead to higher purity material. Some experiments are planned to confirm this hypothesis.

4 Target composition

Some experiments have been performed with the best conditions deduced from the preceding observations (pressure in the range 500–600 mbar and low flow rate), for various target composition, nature and relative concentration of catalyst elements. The characterization of the produced single wall nanotubes are performed both by electron microscopy (SEM and TEM) and Raman scattering, in terms of purity of the sample and tube diameters. The determination of the chirality of the nanotubes require more refined studies like STM, STEM or nanodiffraction study [6,8]. Direct determination of the tube diameter from TEM pictures must be done carefully as the lattice fringe spacing observed along the image of a rope changes with the rotation of the rope around its axis [4] and the measured values must be confirmed by other method. One can also use picture where a bundle curves through the focal plane of the microscope showing a cross-section of the tubes forming the bundle (Fig. 4c). But the

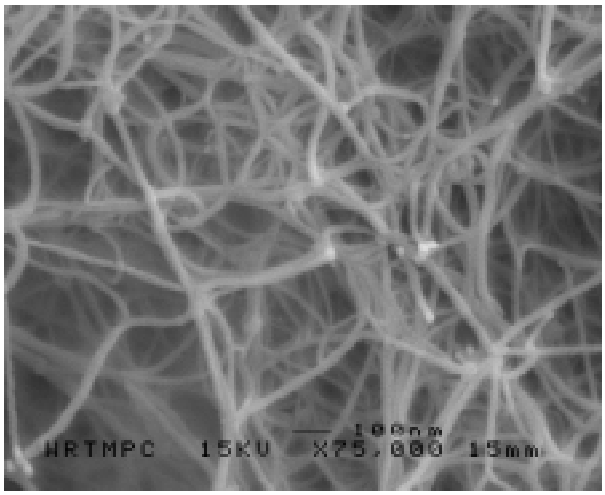

(a)

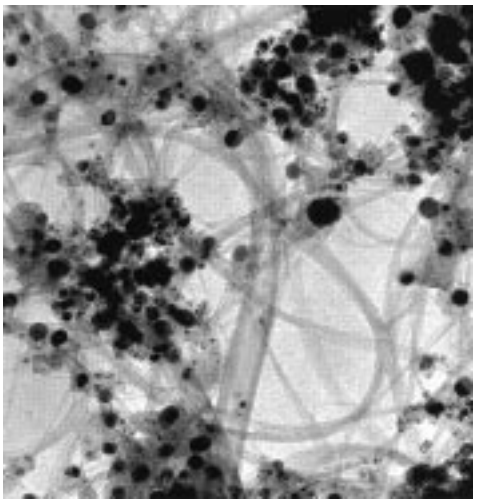

(b)

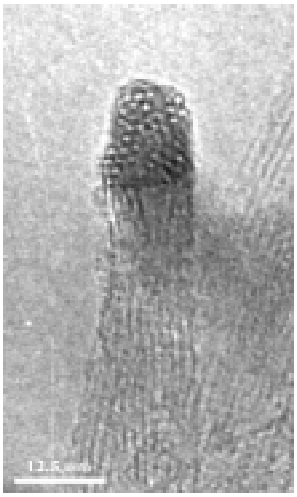

(c)

Fig. 4. The SEM (a) and TEM (b) image of the soot produced at pressure higher than 400 mbar display only bundles of single-wall nanotubes and nanoparticles (same mixture composition as in Fig. 2). HRTEM picture (c) shows the structure of a bundle. In this example, the tube diameter is close to 1.1 nm (HRTEM picture from A. Loiseau, ONERA, France).

number of such cases is small with the used technic of dispersing the sample in ethanol and placing a drop of the material on the grid [9].

The determination of tube diameter can be performed more easily by Raman spectroscopy which is a powerful tool to study the structure of single wall nanotubes. It has been shown that the number of active modes depend only on the type of nanotube: there are 16 expected modes for armchair (n, n) tubes when n is even and 15 modes for all other types [6,10].

Among these modes, the radial breathing mode which appears in the low frequency range (around 180 cm^{-1}) presents a great interest as its frequency is strongly dependent on the tube diameter [11,12], independent of the chirality and follows the linear law $\omega(d) = 223.75/d$ (ω in cm^{-1} and d in nm) as calculated by Bandow *et al.* [13].

If the sample contains tubes with different diameters, the radial breathing band is a superposition of peaks associated with tubes of different diameters. Because of resonant effects, the general shape of this band is also dependent on the frequency of the excitation laser line, different laser line probing preferentially nanotubes with given diameter [14].

The observed Raman spectra of solar produced nanotubes (Fig. 5a) display the general features observed with single-wall nanotubes [15]. In the low frequency range, the Raman spectra of our samples prepared with Ni and Co (Fig. 5b) show a radial breathing band with a large number of peaks, located at frequencies smaller than 180 cm^{-1} corresponding to large diameter tubes. The number of peaks is greater than those observed with samples produced by electric arc or pulsed laser ablation. Using two different excitation lines ($\lambda = 514.5$ nm and $\lambda = 647.1$ nm) one finds that the tubes diameters are in the range 1.7 to 0.9 nm and their chiral vectors fall in the range of the chiral vectors of (12, 12) to (7, 7) armchair nanotubes. This result is in agreement with diameters measured in some unambiguous cases found on the large number of TEM pictures made for these samples. From Raman spectroscopy we also find that the diameter dispersion is weakly dependent of the catalyst concentration in the range 2 at.% to 0.4 at.% of 1/1 mixture. The large distribution of the diameters of nanotubes produced by the solar route can be linked with the large temperature gradient in the formation zone of our reactor. Indeed, recent results [16] from laser ablation method show that the distribution of diameters is broadened as the atmosphere temperature of the reactor decreases because of the increase of the temperature gradient near the target.

Raman experiments performed on tubes produced from mixtures of Ni and Y (Fig. 5c) with two tested compositions (4 at.% Ni/2 at.% Y and 2 at.% Ni/0.5 at.% Y) produced smaller diameter dispersions. We also observed important effects, previously reported [15], with mixtures of Ni and La using either lanthanum chloride (Fig. 5d) or lanthanum oxide as source material. More accurate investigations will be necessary to find a link between experimental conditions during the synthesis and the structure of the nanotubes.

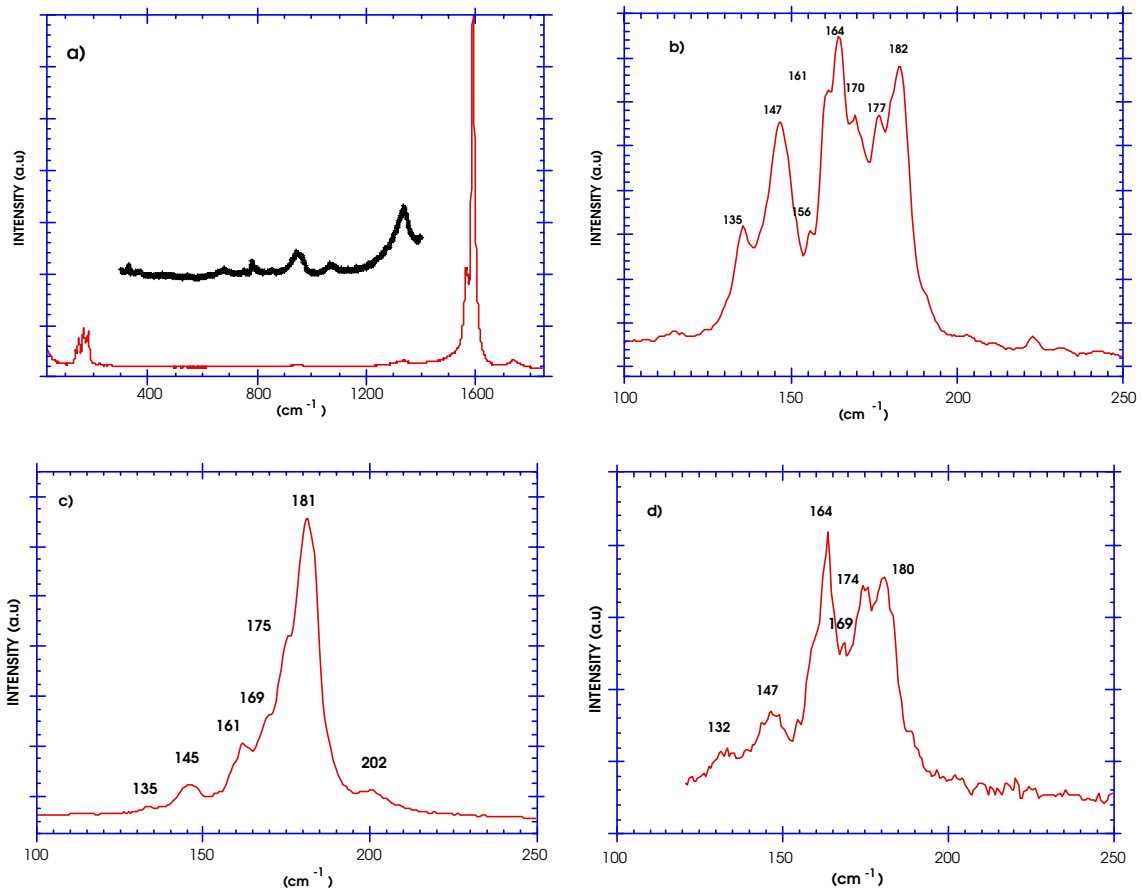

Fig. 5. Raman spectra of carbon nanotubes produced by the solar route. (a, b) Mixture with Ni and Co (2 at.% of 1/1 mixture), (c) mixture with Ni (2 at.%) and Y (0.5 at.%), (d) mixture with Ni (2 at.%) and La (2 at.%, source material Cl_3La). The low frequency range display a great number of peaks at frequencies lower than 180 cm^{-1} which can be interpreted as breathing modes of large diameter single-wall nanotubes.

One must note that the homogeneity of the as-prepared solar samples is poor so that the relative intensity of the Raman peaks can change with the studied area. On the other hand we can observe on TEM images some area with a large number of undesired nanoparticles and amorphous carbon. The presence of amorphous carbon is also pointed out on Raman spectra when one observes a large and smooth peak near 1350 cm^{-1}.

5 Conclusion

This review of the different experiments done with a 2 kW solar furnace shows the numerous advantages of the solar approach. At this time all the synthesis parameters except the vaporization temperature can be adjusted in an independent way. But some improvements are now in progress to remove this problem, one of them being the use of an electric oven to insure a preheating of the targets. A particular advantage of this solar route in contrast to the electric arc method is that non-conducting materials as well as powdered mixture can be easily vaporized.

This study shows the influence of the experimental conditions on the structure of the produced nanotubes and future work will develop a better understanding of the growth mechanisms of these structures. The second goal is the production of large amount of high purity material. A possible way is the use of a larger furnace, like the 1000 kW furnace at the Odeillo Institute. Tests are now in progress to determine if the vaporization of larger targets at higher temperatures can produce large quantities of high purity nanotube structures.

References

1. D. Laplaze, P. Bernier, G. Flamant, M. Lebrun, A. Brunelle, S. Della-Negra, J. Phys. B **29**, 4943 (1996).
2. D. Laplaze, P. Bernier, W.K. Maser, G. Flamant, T. Guillard, A. Loiseau, Carbone **36**, 685 (1998).
3. D. Laplaze, P. Bernier, C. Journet, V. Vié, G. Flamant, E. Philippot, M. Lebrun, *Proceeding of the 8th International Symposium on Solar Thermal Concentrating Technologies*, Cologne, Germany, Oct. 1996, edited by C.F. Muller (Verlag Heidelberg), p. 1653.
4. A. Thess, R. Jee, P. Nikolaev, H. Dai, P. Petit, J. Robert, C. Xu, Y. Hee Lee, S. Gon Kim, A.G. Rinzler, D.T. Colbert, G.E. Scuseria, D. Tomanek, J.E. Fisher, R.E. Smalley, Science **273**, 483 (1996).

5. C.H. Kiang, W.A. Goddard, R. Beyers, D.S. Bethune, Carbon **33**, 903 (1995).
6. R. Saito, G. Dresselhaus, M.S. Dresselhaus, *Physical properties of carbon nanotubes* (Imperial College Press, World Scientific Publishing Co, 1998).
7. M. Yudasaka, T. Komatsu, T. Ichihashi, Y. Achiba, S. Iijima, J. Phys. Chem. B **102**, 4892 (1998).
8. J.M. Cowley, P. Nikolaev, A. Thess, R.E. Smalley, Chem. Phys. Lett. **265**, 379 (1997).
9. S.L. Fang, A.M. Rao, P.C. Eklund, P. Nikolaev, A.G. Rinzler, R.E. Smalley, J. Mater. Res. **13**, 2405 (1998).
10. M.S. Dresselhaus, G. Dresselhaus, P.C. Eklund, in *Science of fullerenes and carbon nanotubes* (Academic Press Inc, New-York, 1996).
11. P.C. Eklund, J.M. Holden, R.A. Jishi, Carbon **33**, 959 (1995).
12. A.M. Rao, E. Richter, S. Bandow, B. Chase, P.C. Eklund, K.A. Williams, S. Fang, K.R. Subbaswamy, M. Menon, A. Thess, R.E. Smalley, G. Dresselhaus, M.S. Dresselhaus, Science **275**, 187 (1997).
13. S. Bandow, S. Asaka, Y. Saito, A.M. Rao, L. Grigorian, E. Richter, P.C. Eklund, Phys. Rev. Lett. **79**, 2738 (1998).
14. M.A. Pimenta, A. Marucci, S.D.M. Brown, M.J. Matthews, A.M. Rao, P.C. Eklund, R.E. Smalley, G. Dresselhaus, M.S. Dresselhaus, J. Mater. Res. **13**, 2396 (1998).
15. E. Anglaret, N. Bendiab, T. Guillard, C. Journet, G. Flamant, D. Laplaze, P. Bernier, J.L. Sauvajol, Carbon **36**, 1815 (1998).
16. M. Yudasaka, T.Ichihashi, Y. Achiba, S. Iijima, *Eurocarbon'98*, Strasbourg, July 1998 (extended Abstract, p. 863).